JOURNAL OF MATERIALS SCIENCE 20 (1985) 399–406

Dynamic compaction of amorphous $Ni_{75}Si_8B_{17}$ and $Pd_{78}Cu_6Si_{16}$ alloys

T. NEGISHI*, T. OGURA, T. MASUMOTO, T. GOTO†, K. FUKUOKA, Y. SYONO
The Research Institute for Iron, Steel and Other Metals, Tohoku University, Sendai, Japan

H. ISHII
Riken Co, Kudankita, Chiyodaku, Tokyo, Japan

Amorphous $Ni_{75}Si_8B_{17}$ and $Pd_{78}Cu_6Si_{16}$ alloy powders were dynamically compacted using a propellant gun. The degree of compaction increases with increase in the magnitude of shock pressure. The shock pressure giving the highest degree of compaction is lower in $Pd_{78}Cu_6Si_{16}$ than in $Ni_{75}Si_8B_{17}$. The progress of compaction-induced crystallization is faster in $Pd_{78}Cu_6Si_{16}$ than in $Ni_{75}Si_8B_{17}$, reflecting the difference in their exothermic characteristics during heating. Evidence was found for a melting and solidification mechanism of dynamic compaction of amorphous powders.

1. Introduction

Rapid quenching of molten metallic alloys allows us to obtain amorphous metals having various chemical compositions and various mechanical, chemical, and electro-magnetic properties [1]. The amorphous metals obtained by such liquid-quenching methods, however, can take only a limited number of shapes: thin ribbons [2, 3], wires [4] and powders [5]. This limitation is a major barrier against the spread of the amorphous metals over a wider industrial field. It appears natural to think of the consolidation of amorphous powders as a means of obtaining bulky amorphous metals.

Several trials have been undertaken to consolidate amorphous powders using explosive or gas gun techniques [6–11]. In such dynamic ways, extremely high pressures (several GPa) can be loaded on to powders for extremely short times (several microseconds). The mean temperature of the powders is expected to be kept well below their crystallization temperatures throughout the course of the compacting procedure. It has been reported that the hardness of dynamically compacted powders reaches the same level as that of the original amorphous ribbons [9], but that the toughness falls to about only one-third of that of the original ribbons [8].

In order to improve the properties of dynamically compacted amorphous powders, it is necessary to unveil details of the process of dynamic compaction and to examine the effects of compacting conditions on the properties of the compacted materials. In the present study, efforts were made to dynamically compact some amorphous alloy powders under a wide range of shock pressures. Special attention is focussed on the degree of consolidation, as well as on the crystallization accompanying the process of dynamic compaction.

2. Experimental methods

The materials selected are amorphous $Ni_{75}Si_8B_{17}$ and $Pd_{78}Cu_6Si_{16}$ alloys, which are obtainable relatively readily, and their basic physical properties have been examined. Amorphous ribbons, about 1 mm wide by about 30 μm thick, were made in air using a single roller melt-quenching apparatus and chopped into pieces about 0.5 to 3.0 mm long. This flaky sample is referred to as

*Present address: Semi-Conductor Division, Atsugi Plant, Sony Co, Atsugi, Japan.
†Present address: The Institute for Solid State Physics, the University of Tokyo, Minato-ku, Tokyo, Japan.

0022–2461/85 $03.00 + .12

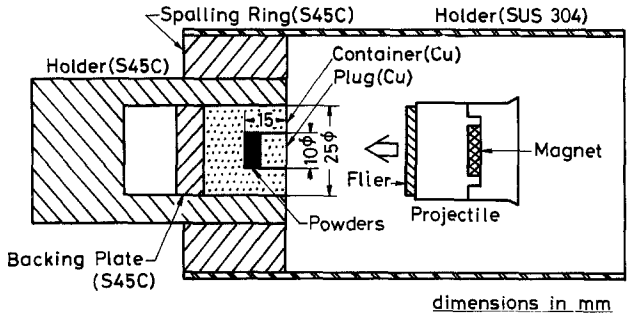

Figure 1 Schematic illustration of the setting for dynamic compaction and the collection of compacted powders.

f-NiSiB when made with the $Ni_{75}Si_8B_{17}$ ribbons, or f-PdCuSi when made with the $Pd_{78}Cu_6Si_{16}$ ribbons. From the $Pd_{78}Cu_6Si_{16}$ alloy, a sample for consolidation was also prepared using a cavitation method with a water-quenching bath [5]. The granular sample, 0.1 to 0.3 mm diameter (48 to 150 mesh), thus obtained is referred to as g-PdCuSi.

Dynamic compaction was performed using a 25 mm bore propellant gun [12], which is capable of accelerating a 20 g projectile to the velocity of 2.3 km sec^{-1}. As illustrated in Fig. 1, 2 to 3 g of the sample powders were put into a container and kept pressed with a plug under a constant static pressure of 0.2 GPa. A high velocity flier plate glued onto a plastic projectile was accelerated by the propellent gun to collide with the top surface of the container placed in a vacuum chamber. The shock pressure produced by the impact can be controlled by the speed of the projectile and the material of the flier: plastics, aluminium or stainless steel. The magnitude of the shock pressure was calculated by the impedance-matching technique [13] from the measured projectile velocity and the Hugoniots of the materials involved in the collision. Since the Hugoniots of the amorphous powders as packed into the container have not been determined, the shock pressure produced in the plug (copper) was calculated, and is tentatively used in the present paper as a measure of the shock pressure loaded on to the amorphous samples.

The degree of compaction and the strength of cohesion of the compacted particles were evaluated by measuring the density and the hardness of compacted powders. The density measurement was made by applying the Archimedean method. When many gaps between compacted particles remained in the surface of the compacted block, density was measured after removing the surface gaps. In the measurement of hardness, a Knoop indenter was pressed on to the mechanically polished cross-section of the compacted block in such a way that the longer diagonal was normal to the trace of the interface of compacted particles. When the cohesion strength of compacted particles is small, failure and sliding take place along the interface existing beneath the Knoop indenter, and depress the apparent hardness values. Ten hardness measurements were made with a given sample and the results were averaged.

The crystallization of the amorphous samples due to heat generation during dynamic compaction was examined using both an X-ray diffractometer (Cu$K\alpha$, 35 kV, 15 mA) and a differential scanning calorimeter (DSC). The standard material and the heating speed in the DSC analysis were lead and 40 K min^{-1}, respectively. Crystallization in f-NiSiB was also examined by chemical etching using a solution prepared from 20 ml 60% $HClO_4$ and several ml 30% H_2O_2. It has been confirmed that only the crystalline $Ni_{75}Si_8B_{17}$ is sensitive to the etching solution.

3. Experimental results

3.1. Dynamic compaction and compaction-induced crystallization in f-NiSiB

Mechanically polished cross-sections of f-NiSiB dynamically compacted under various shock pressures are shown in Fig. 2. Traces of interfaces between compacted flakes are seen more clearly for samples which suffered lower shock pressures, suggesting that the higher the shock pressure, the better is the degree of compaction. The packing density before compaction has been measured as 6.5 $Mg\,m^{-3}$. The density of compacted f-NiSiB has been found to increase with increase in shock pressure and to reach 7.7 $Mg\,m^{-3}$ at a shock pressure of 20 GPa. This value is 97% of the

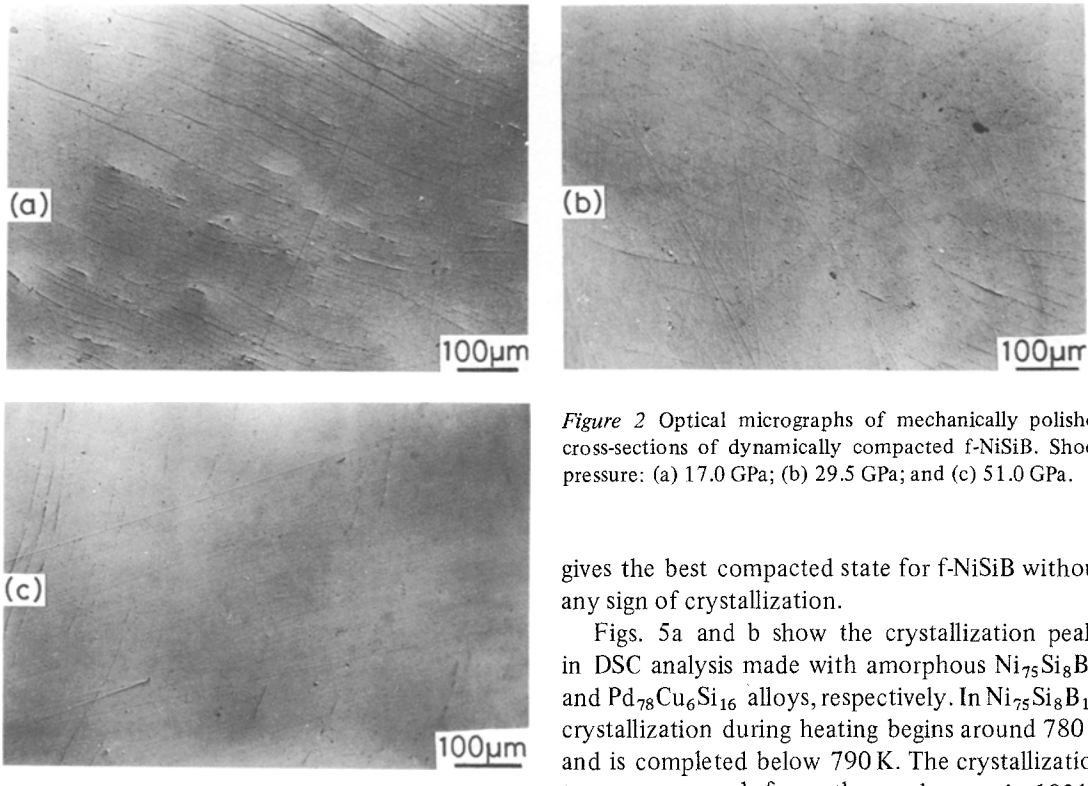

Figure 2 Optical micrographs of mechanically polished cross-sections of dynamically compacted f-NiSiB. Shock pressure: (a) 17.0 GPa; (b) 29.5 GPa; and (c) 51.0 GPa.

density of the original amorphous ribbons and as high as those obtained with dynamically compacted amorphous $Ni_{57}Mo_{23.5}Fe_9B_{10.5}$ [9] and $Nb_{40}Fe_{40}P_{14}B_6$ [8] alloys.

Plots of the Knoop hardness against shock pressure are shown in Fig. 3. The hardness of the original amorphous ribbons and that of fully crystallized ribbons are also shown for comparison. The hardness obtained under shock pressures less than 25 GPa are below the level of the hardness of the original amorphous ribbons. This indicates that the cohesion of the interface between compacted flakes is not so strong that the interface separation and mutual sliding of adjacent flakes occur beneath the Knoop indenter. It is probable that the compaction-induced crystallization takes place above 35 GPa.

The results of X-ray diffraction made with dynamically compacted f-NiSiB are shown in Fig. 4. Compaction-induced crystallization is easily recognized when the shock pressure reaches 35 GPa. Every crystalline peak seen in the figure is identified as either equilibrium Ni_3B or Ni_3Si. From Figs. 3 and 4 it is suggested that the compaction under a shock pressure of around 30 GPa gives the best compacted state for f-NiSiB without any sign of crystallization.

Figs. 5a and b show the crystallization peaks in DSC analysis made with amorphous $Ni_{75}Si_8B_{17}$ and $Pd_{78}Cu_6Si_{16}$ alloys, respectively. In $Ni_{75}Si_8B_{17}$, crystallization during heating begins around 780 K and is completed below 790 K. The crystallization energy measured from the peak area is 102 kJ kg^{-1}. In $Pd_{78}Cu_6Si_{16}$, crystallization begins around 685 K, proceeds gradually, and is completed at about 710 K. The average crystallization energy is 31 kJ kg^{-1}. Thus, crystallization in the latter starts at a lower temperature, proceeds more gradually, and is a much easier transition phenomenon compared with that in the former.

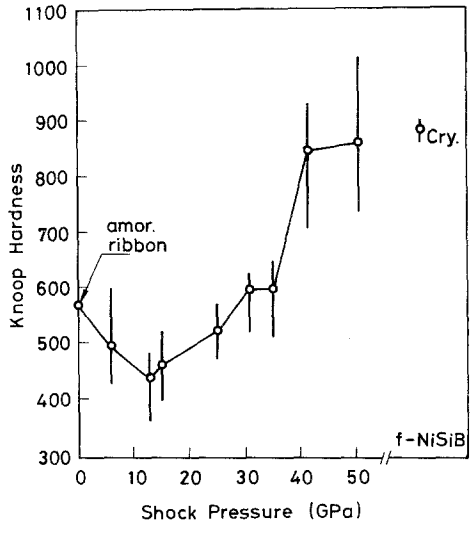

Figure 3 Change in the Knoop hardness of dynamically compacted f-NiSiB with shock pressure.

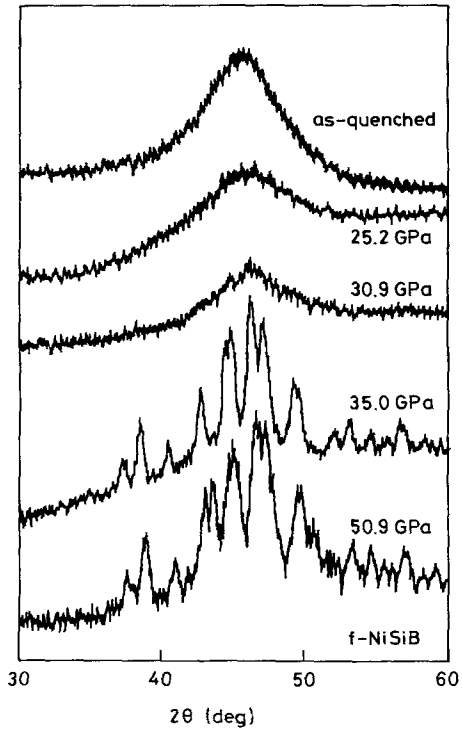

Figure 4 X-ray diffraction patterns obtained from dynamically compacted f-NiSiB.

The result of DSC analysis of dynamically compacted f-NiSiB is shown in Fig. 6 as plots of specific calorific value, ΔH, against shock pressure. A sharp decrease in ΔH is seen as the shock pressure increases from 25 to 35 GPa, confirming that crystallization is completed during the compaction under shock pressures larger than 35 GPa. This DSC result is consistent with the results of X-ray analysis (Fig. 4) and of hardness measurements (Fig. 3). A fairly large decrease in ΔH below 30.9 GPa is supposed to be due to such a kind of recovery as gives no sign of crystallization on the X-ray diffraction pattern.

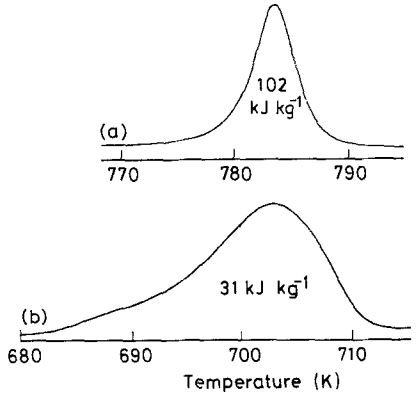

Figure 5 DSC curves (crystallization peaks) of amorphous (a) $Ni_{75}Si_8B_{17}$ and (b) $Pd_{78}Cu_6Si_{16}$ alloys.

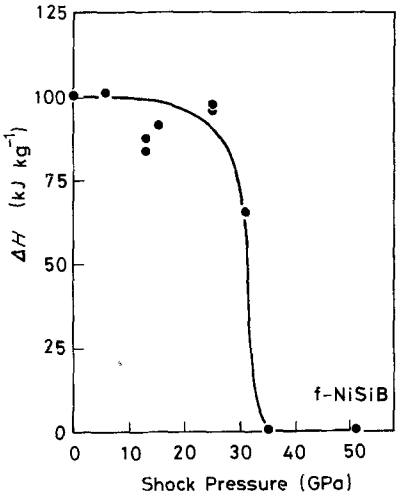

Figure 6 Results of DSC analysis showing the change in the specific calorific value, ΔH, of dynamically compacted f-NiSiB with shock pressure.

3.2. Dynamic compaction and compaction-induced crystallization in f-PdCuSi and g-PdCuSi

Mechanically polished cross-sections of dynamically compacted f-PdCuSi are shown in Fig. 7. Similarly for the case of f-NiSiB, the degree of compaction increases with increase in shock pressure. The density of compacted f-PdCuSi has been found to reach almost the same level as that of the original amorphous ribbons at a shock pressure of 15.8 GPa. Comparing Fig. 7 with Fig. 2, one may easily see that the shock pressure at which a good degree of compaction is attained in f-PdCuSi is much lower than that in f-NiSiB. To visualize better the effect of shock pressure on the degree of compaction in g-PdCuSi, an unusually large quantity of sample powder was packed into the container and given an impact to a shock pressure of 30.2 GPa. The mechanically polished cross-section of the bottom part of the compacted block is shown in Fig. 8, where the arrow in the upper left-hand corner indicates the direction of shock wave propagation. One sees that the thickness of the as-packed sample was too large for the shock wave to propagate through without appreciable attenuation, and that a higher shock pressure guarantees a better degree of

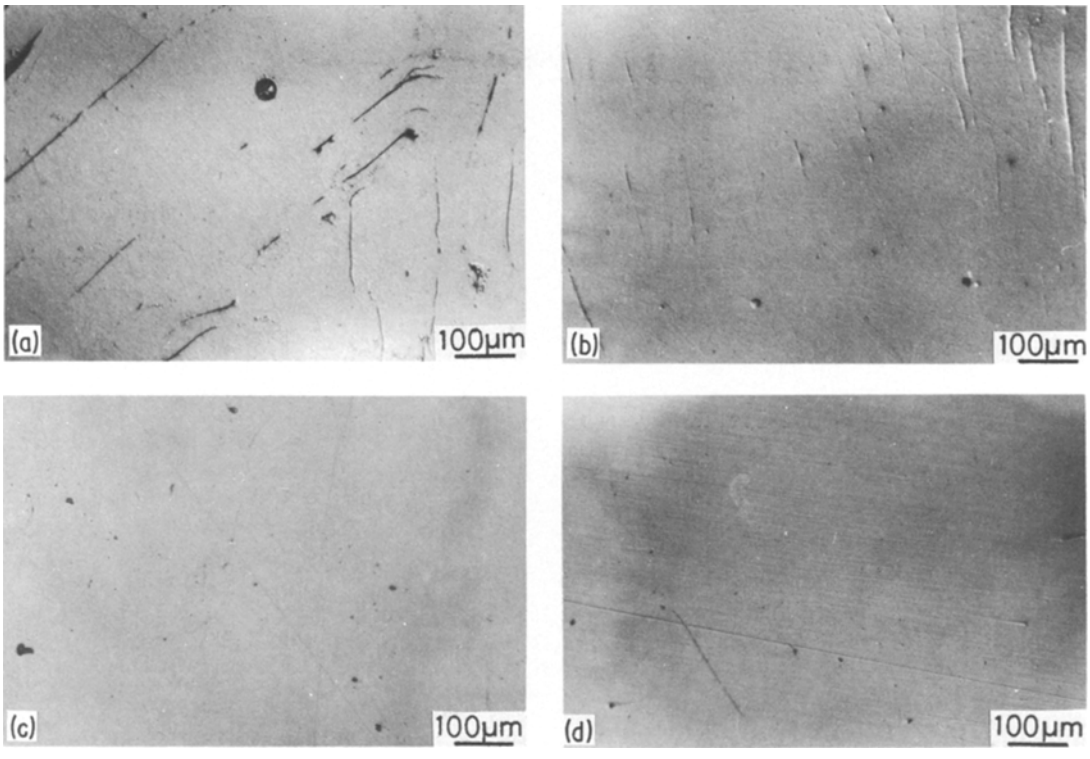

Figure 7 Optical micrographs of mechanically polished cross-sections of dynamically compacted f-PdCuSi. Shock pressure: (a) 11.7 GPa; (b) 15.8 GPa; (c) 24.8 GPa; and (d) 36.4 GPa.

compaction. Spherical holes, such as those marked by the letter H, existing in the perfectly compacted region indicate that melting occurred there. It is interesting to note that grain interfaces perpendicular to the direction of shock wave propagation are more readily visible in the imperfectly compacted region; sticking of two grains occurs more easily at such interfaces which are parallel to the direction of shock wave propagation. From this finding it is suggested that mechanical friction at interfaces plays an important role in the bonding process of particles under relatively low shock pressures.

The relationship between the Knoop hardness of compacted f-PdCuSi or g-PdCuSi and shock pressure is shown in Fig. 9. Similarly in f-NiSiB, the apparent hardness of compacted f-PdCuSi is smaller than the hardness of the original ribbons

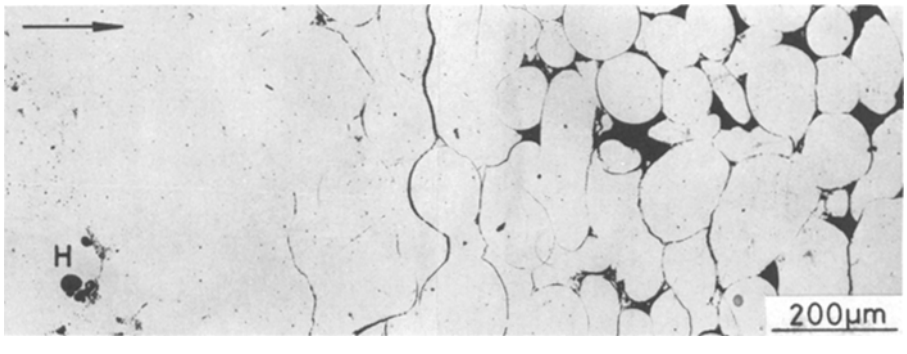

Figure 8 An optical micrograph of the mechanically polished cross-section of g-PdCuSi dynamically compacted under a shock pressure of 30.2 GPa. The attenuation of shock pressure resulted in the change in the degree of compaction along the direction of shock wave propagation.

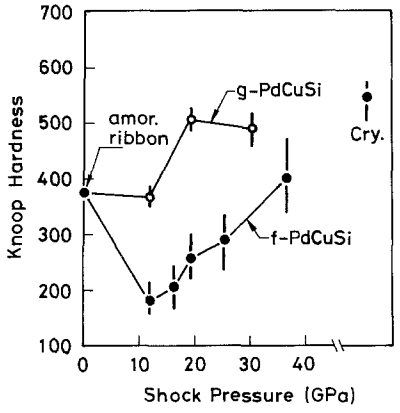

Figure 9 Change in the Knoop hardness of dynamically compacted f-PdCuSi and g-PdCuSi with shock pressure.

in a range of lower shock pressures. In the case of g-PdCuSi, such a decrease in hardness has not been detected. It is evident that the shock pressure at which hardness recovers to the original level is much larger in f-PdCuSi than in g-PdCuSi; g-PdCuSi is compacted more easily than f-PdCuSi.

The results of X-ray diffraction made with dynamically compacted f-PdCuSi are shown in Fig. 10. Crystallization appears to have already taken place at 15.8 GPa, which is far below the corresponding shock pressure of f-NiSiB (Fig. 4).

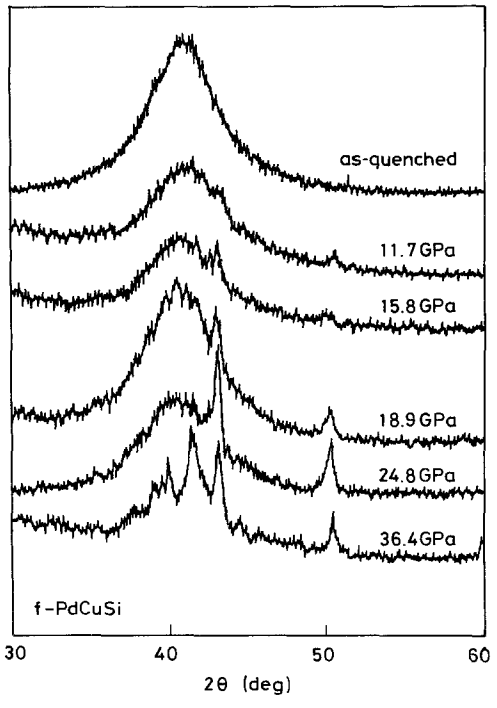

Figure 10 X-ray diffraction patterns obtained from dynamically compacted f-PdCuSi.

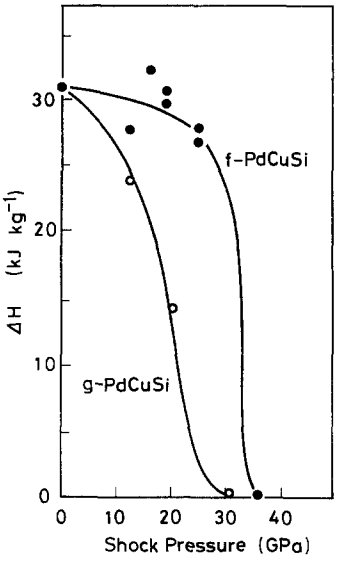

Figure 11 Results of DSC analysis showing the change in the specific calorific value, ΔH, of dynamically compacted f-PdCuSi with shock pressure.

However, an evident amorphism still remains at 24.8 GPa. The crystallization behaviour of f-PdCuSi is thus quite different from that of f-NiSiB. This is attributed to the difference in the exothermic characteristics of the two amorphous materials during heating (Fig. 5).

Specific calorific values obtained with f-PdCuSi and g-PdCuSi are plotted against shock pressures in Fig. 11. It is evident that the amount of recovery at a fixed shock pressure is larger for g-PdCuSi compared with that of f-PdCuSi, suggesting that the heat generation during dynamic compaction is more intense in g-PdCuSi than in f-PdCuSi. This DSC result is consistent with the results of hardness measurements (Fig. 9) and of X-ray analysis (Fig. 10).

4. Discussion

In the as-packed state of amorphous powders, a certain amount of porosity is always present depending upon the size and shape of the powder particles and the magnitude of the static pressure being loaded on to the packed powders. There also exists a high concentration of micro-scale voids or gaps in the interface of two contacting particles, since the surface of any particle is never ideally flat. Sharp heat generation is then expected to occur selectively in the interfaces during the passage of shock waves, due to mechanical friction and/or adiabatic plastic flow accompanying

mutual sliding and high speed collision of adjacent particles through which the porosities and the micro-scale voids become solid. Under a given shock pressure, more heat generation is expected in more loosely packed powders, since the mechanical friction and adiabatic plastic flow would occur in a larger scale. Plate-like powders having a smaller aspect ratio may be favorable for bonding via the friction mechanism as suggested in Fig. 8. In the light of these considerations, the difference in the behaviours in dynamic compaction and compaction-induced crystallization between f-PdCuSi and g-PdCuSi (Figs. 9, 10, and 11) is well understood, since the packing density of f-PdCuSi (about 83% of the density of the original ribbons), is higher than that of g-PdCuSi (about 75%). It is also noticeable that the aspect ratio of f-PdCuSi is much larger than the "effective" aspect ratio of g-PdCuSi.

The duration time for which particles are kept under a shock pressure is of the order of $2d/U_s$, d and U_s being the thickness of flier and the speed of the shock wave in the flier material, respectively, and estimated to be several microseconds, assuming d and U_s to be about 3 mm and several km sec^{-1}, respectively. Hence one may see that the heat generation at the particle interfaces is made over an extremely short time. If the temperature of the interfaces rise above melting point, the interfaces are filled with molten metal. If the molten metal is chilled sufficiently fast by the cold bulk, it becomes amorphous solid again. This is a melting and solidification mechanism proposed for the dynamic compaction of amorphous powders on the basis of structural observations on dynamically compacted tool steel powders [14]. However, the mechanism seems to be not necessarily supported by ample experimental evidence. It is expected that, under the same compacting conditions, powders having a lower melting point should be compacted well under a lower shock pressure. Then, the fact that f-PdCuSi was well compacted under lower shock pressures than f-NiSiB (Figs. 2 and 7) is consistent with the above mechanism, since the melting point of the former, 1029 K [15], is much lower than that of the latter, 1340 K [16].

Further evidence for the melting and solidification mechanism is given below. During the course of examining the crystallization behaviour in f-NiSiB by means of the chemical etching method, we have found that crystallized islands

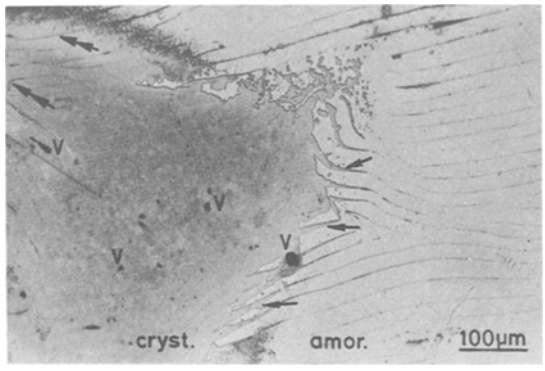

Figure 12 An example of a crystallized island etched out in f-NiSiB dynamically compacted under a shock pressure of 30.9 GPa.

were sometimes formed in the compacted amorphous matrix. The formation of such islands is attributed to non-uniformity in the packing density of f-NiSiB of which the aspect ratio is too large to be packed uniformly. A region of extremely low packing density generates a very large amount of heat upon compaction, melts, and becomes a crystallized island after resolidification. Part of an island found in f-NiSiB compacted under 30.9 GPa is shown in Fig. 12, where the island is easily recognized as a selectively etched region. Note that the compaction under a shock pressure of 30.9 GPa, gave the best compacted state without appreciable crystallization (Fig. 3). Small spherical voids marked by the letter V existing in the island indicate that at least a part of this region melted and resolidified. It is interesting to note that the island penetrated into nearby interfaces between compacted flakes (arrows). This observation suggests that localized and preferential temperature rise and melting occurred in the interfaces between flakes.

It has been found that flake-interfaces in compacted samples are easily etched out, even when they are not visible in mechanically polished cross-sections. Such a special sensitivity of the interfaces to chemical etching may be caused by the existence of filmy non-amorphous substances such as metal oxides and/or crystallized phases. The existence of substances other than crystallized phases is confirmed by the fact that the interfaces in the crystallized island are sometimes sensitive to chemical etching (see double arrow in Fig. 12). It is emphasized that the crystallized island as well as the filmy substances left in the flake-interfaces must be the origin of

deterioration of various properties of compacted amorphous powders. Material factors which may be taken into account in order to obtain better compacted amorphous powders are, therefore:

1. The size of powders must be fine enough to ensure uniform packing in the container, but it must be large enough to ensure rapid solidification of melt produced in the interfaces;

2. the surface of the powders must be finished as clean as possible; and

3. amorphous powders having smaller aspect ratios are desirable to ensure uniform packing as well as easier bonding via friction mechanisms.

5. Conclusion

Amorphous $Ni_{75}Si_8B_{17}$ (flaky: f-NiSiB) and $Pd_{78}Cu_6Si_{16}$ (flaky: f-PdCuSi; granular: g-PdCuSi) alloys were dynamically compacted using a propellant gun under various levels of shock pressure. The effect of the magnitude of the shock pressures on the degree of compaction and on the compaction-induced crystallization was examined by means of hardness and density measurements, X-ray diffraction, and DSC. The results are summarized as follows.

1. In both f-NiSiB and f-PdCuSi, the degree of compaction increases with increase in shock pressure. The magnitude of the shock pressure which gives the highest degree of compaction under the present conditions is larger for f-NiSiB than for f-PdCuSi.

2. In f-NiSiB the compaction-induced crystallization begins at about 30 GPa and is completed at about 35 GPa. In f-PdCuSi it begins at about 16 GPa and is completed at about 35 GPa. The difference in the crystallization behaviour between the two materials reflects the difference in their exothermic behaviour during heating.

3. g-PdCuSi, having a lower packing density compared with f-PdCuSi, is compacted well at lower shock pressures than f-PdCuSi. The progress of compaction-induced crystallization is much faster in g-PdCuSi than in f-PdCuSi.

4. Evidence is shown for the melting and solidification mechanism of the dynamic compaction of amorphous powders, and the size and the shape of amorphous powders which may give better compacted powders is briefly discussed.

References

1. T. MASUMOTO, Proceedings 4th International Conference on Rapidly Quenched Metals (RQ4) Vol. 1, (The Japan Institute of Metals, 1982) p. 5.
2. R. POND and R. MADDIN, *Trans. AIME* **245** (1969) 407.
3. T. MASUMOTO and R. MADDIN, Proceedings International Conference on Metastable Metallic Alloys (Brela, Yugoslavia, 1970).
4. T. MASUMOTO, I. OHNAKA, A. INOUE and M. HAGIWARA, *Scripta Metall.* **15** (1981) 293.
5. H. ISHII, M. NAKA and T. MASUMOTO, *Sci. Rep. RITU* **A29** (1981) 343.
6. C. F. CLINE and R. HOPPER, *Scripta Metall.* **11** (1977) 1137.
7. D. RAYBOULT, D. G. MORRIS and G. A. COPPER, *J. Mater. Sci.* **14** (1979) 2523.
8. D. G. MORRIS, *Met. Sci.* **14** (1980) 215.
9. C. F. CLINE, Proceedings 4th International Conference on Rapidly Quenched Metals (RQ4), Vol. 1 (The Japan Institute of Metals, 1982) p. 129.
10. D. G. MORRIS, *ibid.*, p. 145.
11. O. V. ROMAN, V. G. GOROTSOV, B. S. MITIN and V. A. VASILYEV, *ibid.* p. 149.
12. Y. SYONO and G. GOTO, AIP Conference Proceedings No. 78 (American Institute of Physics, 1982) p. 701.
13. J. M. WALSH and R. H. CHRISTIAN, *Phys. Rev.* 97 (1955) 1544.
14. D. G. MORRIS, *Met. Sci.* **15** (1981) 116.
15. M. NAKA, Y. NISHI and T. MASUMOTO, Proceedings 3rd International Conference on Rapidly Quenched Metals (RQ3), Vol. 1 (The Metals Society, 1978) p. 231.
16. R. A. GRANGE and J. M. KIEFER, *Trans. ASM* 29 (1941) 85. cited in D. G. MORRIS, *Acta Metall.* **31** (1983) 1479.

Received 22 February
and accepted 9 March 1984